Terahertz Behavior of Optical Components and Common Materials

Andrew J. Gatesman[*a], Andriy Danylov[a], Thomas M. Goyette[a], Jason C. Dickinson[a], Robert H. Giles[a], William Goodhue[a], Jerry Waldman[a], William E. Nixon[b], and Weber Hoen[c]

[a] Submillimeter-Wave Technology Laboratory
University of Massachusetts Lowell
Lowell, MA 01854

[b]U.S. Army National Ground Intelligence Center
Charlottesville, VA 22911

[c]Aerospace Sensor Technology
Lincoln Laboratory
Massachusetts Institute of Technology
Lexington, MA 02420

ABSTRACT

As short range, ground based, surveillance systems operating at terahertz frequencies continue to evolve, increasing attention is being directed towards the behavior of dielectric materials at terahertz frequencies as well as the behavior of optical components used to control terahertz radiation. This work provides an overview of several terahertz optical components such as frequency selective filters, laser output couplers, artificial dielectrics, and electromagnetic absorbers. In addition, a database was established that contains terahertz properties of common materials that have been largely unexplored in this region of the spectrum. The database consists of transmittance and reflectance spectra of a variety of materials measured using Fourier transform infrared spectroscopy techniques from 175 GHz - 2 THz. In addition, ultra-stable, CO_2 optically pumped, far-infrared gas lasers were used to collect fixed-frequency transmittance data at 326 GHz, 584 GHz, and 1.04 THz. A Gunn oscillator was used for measurements at 94 GHz.

Keywords: THz, materials, dielectric, absorbers, attenuation

1. INTRODUCTION

Since 1981, Expert Radar Signature Solutions (ERADS) under funding from the U.S. National Ground Intelligence Center (NGIC), has developed state-of-the-art compact radar ranges operating at terahertz (THz) frequencies in support of operational radars and a number of advanced radar applications such as assisted target recognition systems, radar absorbing materials development, and obscured object detection. ERADS has developed fully polarimetric compact ranges at 6-18 GHz[1], 160 GHz[2], 350 GHz[3], 520 GHz[4], and 1.56 THz[5] for acquisition of UHF, X, Ka, and W-band radar imagery of 1/16th and 1/35th scale model targets situated in free-space and cluttered environments.

[*] correspondence: email: andrew_gatesman@uml.edu; telephone: 978-934-1365; fax: 978-452-3333

Report Documentation Page

Form Approved
OMB No. 0704-0188

1. REPORT DATE	2. REPORT TYPE	3. DATES COVERED
MAY 2006		**00-00-2006 to 00-00-2006**

4. TITLE AND SUBTITLE	5a. CONTRACT NUMBER
Terahertz Behavior of Optical Components and Common Materials	5b. GRANT NUMBER
	5c. PROGRAM ELEMENT NUMBER
6. AUTHOR(S)	5d. PROJECT NUMBER
	5e. TASK NUMBER
	5f. WORK UNIT NUMBER
7. PERFORMING ORGANIZATION NAME(S) AND ADDRESS(ES) **University of Massachusetts Lowell,Submillimeter-Wave Technology Laboratory,175 Cabot Street,Lowell,MA,01854**	8. PERFORMING ORGANIZATION REPORT NUMBER
9. SPONSORING/MONITORING AGENCY NAME(S) AND ADDRESS(ES)	10. SPONSOR/MONITOR'S ACRONYM(S)
	11. SPONSOR/MONITOR'S REPORT NUMBER(S)

12. DISTRIBUTION/AVAILABILITY STATEMENT
Approved for public release; distribution unlimited

13. SUPPLEMENTARY NOTES
The original document contains color images.

14. ABSTRACT

15. SUBJECT TERMS

16. SECURITY CLASSIFICATION OF:			17. LIMITATION OF ABSTRACT	18. NUMBER OF PAGES	19a. NAME OF RESPONSIBLE PERSON
a. REPORT	b. ABSTRACT	c. THIS PAGE			
unclassified	**unclassified**	**unclassified**		**12**	

In order to acquire realistic radar signatures using scale modeling techniques, the dielectric properties of non-metallic target components must be appropriately scaled. The necessary THz dielectric scaling technology[6] has been developed to properly model non-metallic components of the targets. In addition to the development of artificial dielectrics, the establishment of THz radar signature measurement systems also required the development of a variety of specialized optical components, as well as the ability to characterize these structures.

Recently, there has been an increase in interest to develop short range, ground based, surveillance systems at THz frequencies. The Submillimeter-Wave Technology Laboratory (STL) is investigating THz remote sensing systems with the ability to detect obscured objects such as a concealed firearm. Successful development of THz radar and security related applications requires comprehensive knowledge of the optical properties of a wide range of materials and components. This paper describes the optical properties of components of interest to the THz community such as artificial dielectrics, bandpass filters, frequency selective surfaces, and resistive sheets. In addition, the THz transmittance and attenuation behavior of common materials such as clothing, fabric, and building materials are presented.

1.1. Overview of Materials Characterization Capability

The Submillimeter-Wave Technology Laboratory operates and maintains several measurement systems to characterize a material's reflectance and transmittance in the frequency region from 40 MHz through 225 THz. Several of the systems are capable of determining the material's complex dielectric constant. A summary of the current capabilities of these systems is given in Table I.

Table I. Summary of Materials Characterization Capability.

Band	Technique	Frequency range
RF/microwave	coaxial airline, coaxial probe	40 MHz - 20 GHz
microwave	waveguide techniques	8 GHz - 40 GHz
microwave / millimeter-wave	free-space, spot focusing horns	8-12 GHz, 26-40 GHz, 75-110 GHz
millimeter-wave	backward wave oscillators	80-180 GHz
millimeter-wave / terahertz	THz lasers	≈ 200 GHz - 3 THz
millimeter-wave / infrared	Fourier transfom spectroscopy	180 GHz - 225 THz

Coaxial airline techniques and a coaxial probe, based on a vector network analyzer, are used to analyze the 40 MHz - 20 GHz behavior of materials. The network analyzer is also utilized in reflection and transmission measurement systems at X, Ka, and W-bands. Both waveguide and free-space configurations are possible. Free-space measurement capability also includes an 80-180 GHz system based on two backward wave oscillators. Data can be analyzed to determine the complex dielectric constant of the material under test. A Bruker IFS 66vs Fourier transform spectrometer is utilized to measure the reflection and transmission behavior of materials. A variety of sources, detectors, and beamsplitters are available to cover a bandwidth ranging from 180 GHz - 225 THz. Data can be analyzed to determine the material's frequency-dependent complex dielectric constant. The system, operating with a resolution of 3 GHz, is also useful for analyzing the absorption behavior of gases (e.g. atmospheric water vapor) and determining the emission spectra of IR-THz sources (e.g. quantum cascade lasers).

2. THz OPTICAL COMPONENTS and SPECIALIZED MATERIALS

2.1. Artificial Dielectrics

An artificial dielectric can be defined as a "natural" material that has been intentionally modified in such a way as to alter its dielectric constant. The capability to control a material's dielectric constant, and hence its reflectivity and absorptivity, is important in scale model radar measurements. Radar modeling imposes a restriction on the material used to fabricate the scale model, namely, that the complex dielectric constant of the material at the scaled frequency be equal to the complex dielectric constant of the full-scale material at the radar frequency. Using dielectric scaling technology[6], the scaled component is fabricated from plastics and silicone-based materials loaded with specific amounts of powdered filling agents (silicon, graphite, aluminum, copper, stainless steel, etc.) to achieve the full-scale dielectric constant at the scaled frequency.

Figure 1a shows the real and imaginary parts of the dielectric constant at 0.52 THz for polyurethane plastic as a function of TransTech barium tetratitanate (D-38) powder loading. D-38 is a low loss, high dielectric constant material used at microwave frequencies. This type of artificial dielectric is suitable for modeling low-loss target components such as the fiberglass panels on a Army HMMWV (Fig. 1b). At 35 GHz, fiberglass has a dielectric constant of $\varepsilon \approx 4.3 + i\ 0.11$. Figure 1a indicates that a loading of 90% would produce an artificial dielectric with a 0.52 THz dielectric constant of $\varepsilon = 4.3 + i\ 0.16$ and would therefore be adequate for modeling the 35 GHz behavior of fiberglass.

(a) (b)

Figure 1. Complex dielectric constant of a D-38 loaded artificial dielectric at 0.52 THz (left) and the 35 GHz properties of fiberglass (right).

Dielectric scaling techniques can also be used to model lossy materials such as soil. Figure 2a shows the real and imaginary parts of the dielectric constant at 1.56 THz for polyurethane plastic as a function of graphite powder loading. Graphite is a high loss material and is suitable for modeling absorptive materials such as field soil. At 95 GHz, soil has a dielectric constant of $\varepsilon \approx 4.1 + i\ 1.7$. Figure 2a indicates that a graphite loading of 8.5% would produce an artificial dielectric with a 1.56 THz dielectric constant of $\varepsilon = 4.2 + i\ 1.6$ and would sufficiently model the 95 GHz behavior of soil.

(a) (b)

Figure 2. Complex dielectric constant of a graphite loaded artificial dielectric at 1.56 THz (left) and the 95 GHz properties of field soil (right).

2.2. Terahertz Bandpass Filters

Thin metallic sheets with a two-dimensional array of apertures have been used for decades as frequency selective surfaces in a variety of quasi-optical applications. Their optical behavior is dictated by the arrangement and shape of the apertures as well as the sheet thickness. Only recently have such structures, also known as dichroic filters, been grouped under the more general category of photonic bandgap structures. Dichroic filters are typically utilized as bandpass or bandstop filters in the microwave-infrared regions of the spectrum. Two of the more common types are rigid hole-drilled metallic plates[7] and flexible sheets[8,9] produced using photolithographic techniques. Hole-drilled filters offer the advantage of being rugged and easy to manufacture. Filters fabricated with photolithographic techniques offer the advantage of being flexible and lightweight. In addition, a wider range of designs is possible.

Figure 3a shows a 0.157-inch-thick hole-drilled filter designed to transmit 349±15 GHz radiation and strongly attenuate radiation at frequencies below 315 GHz. The pattern consists of an array of 0.55-mm-diameter holes arranged in a hexagonal pattern. A Bruker IFS 66vs Fourier transform spectrometer was used to collect the filter's transmittance at THz frequencies and the data are plotted in Figure 3b. The spectrum shows a sharp cut-on feature at ≈ 330 GHz with a relatively high transmittance of ≈ 80% in the passband and virtually no transmittance below 325 GHz. These filters have been successfully used to attenuate the lower sideband in THz sideband generation experiments based on a 326 GHz molecular gas laser system.

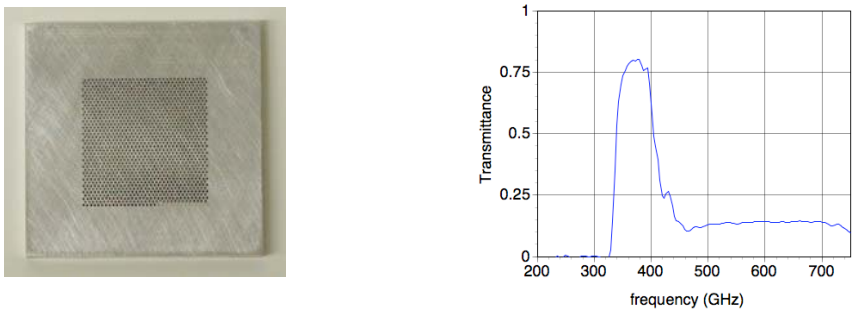

(a) (b)

Figure 3. THz holed-drilled bandpass filter (left) and transmittance spectra (right).

Figure 4a shows a photomicrograph of a 3-inch-diameter, 12-micron-thick, flexible THz bandpass filter. The structure was fabricated using photolithographic and electroplating techniques. The length and width of the crossed-dipole apertures are approximately 400 and 68 microns, respectively, with a periodicity of 700 microns. This filter was also designed with a center frequency of 349 GHz. The filter's transmittance at THz frequencies is plotted in Figure 4b. In contrast to Fig. 3b, the crossed dipole filter transmits 100% at 349 GHz; however, substantially more radiation is transmitted below 315 GHz.

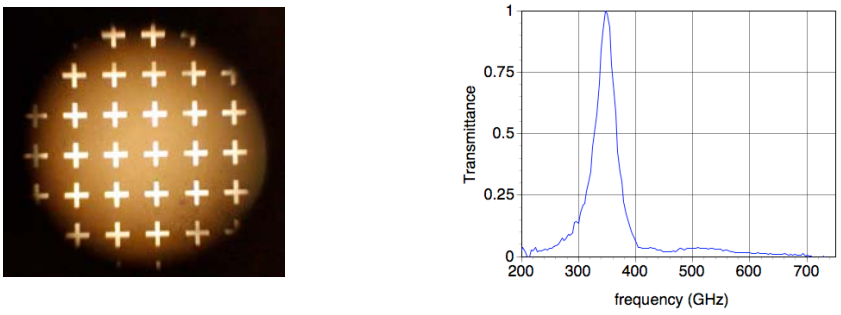

(a) (b)

Figure 4. THz freestanding, crossed-dipole bandpass filter (left) and transmittance spectra (right).

2.3. Terahertz Laser Uniform Output Couplers

Closely related to the filters described in Section 2.2 are the frequency selective surfaces used as uniform output couplers for CO_2-pumped THz molecular gas lasers. These devices are typically 1 - 3 inches in diameter, approximately 2 mm thick, and are based on low-loss substrates upon which several thin dielectric layers are deposited to achieve high reflectivity at the CO_2 pump laser wavelength. High resistivity silicon has been shown to be extremely low loss at THz frequencies[10] and is typically chosen as the substrate material. A metallic mesh or strip pattern is used to achieve a specific reflectivity at terahertz frequencies, typically in the range of 85%-95%. Uniform output couplers have been shown to produce higher THz laser output power and better mode characteristics than traditional hole couplers.[11]

Figure 5a shows a photograph of a strip-type uniform output coupler designed for the 323.90 GHz and 326.11 GHz laser lines in O-deutero formic acid. The pattern was designed using Periodic Method of Moments[12] (PMM) software and consisted of 18-micron wide inductive gold strips with an 80-micron periodicity. The transmittance spectrum is shown in Figure 5b from which the coupler's reflectance can be determined.

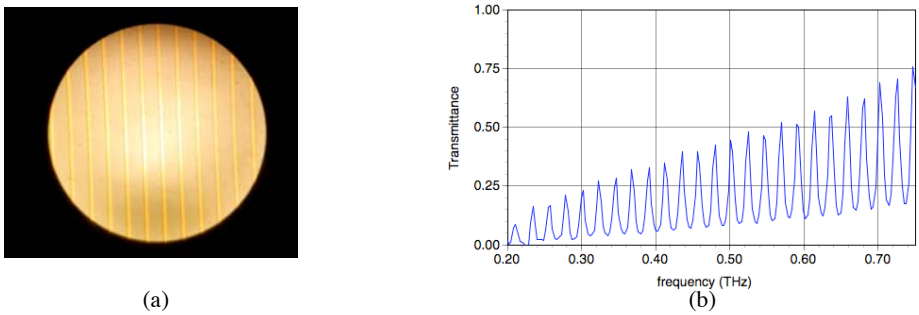

(a) (b)

Figure 5. Strip-type uniform output coupler for a ≈ 325 GHz molecular gas laser (left) and transmission spectra (right).

The rapid oscillation in the coupler's transmittance in Figure 5b is due to the optical behavior of the silicon etalon substrate. This rapid oscillation along with the application of the dielectric stack and metallic pattern make it difficult to predict the coupler's exact behavior prior to fabrication. A finished coupler of the type shown in Figure 5a could have a 325 GHz transmittance that falls anywhere within the ≈ 25% envelope of the above spectra. To get around this dilemma, a post-fabrication process to control the substrate thickness has been successfully demonstrated. The silicon substrate thickness is reduced via a controlled chemical etching technique and has been shown to "tune" the coupler's thickness, and hence its reflectivity, to the appropriate value.[13] Furthermore, when there are more than two THz laser lines present, it is possible to optimize the coupler for one frequency and detune it for the other.

STL also fabricated the output couplers for the 2.5 THz laser local oscillator built by DeMaria ElectroOptic Systems (DEOS) for the NASA AURA satellite program. These space-qualified optics were printed with a Au capacitive mesh-type pattern (Fig. 6a) to achieve ≈ 10% transmittance (i.e. 90% reflectance) at the 118.83 micron THz laser line in methyl alcohol (Fig. 6b). The uniform output coupler enabled DEOS to achieve greater than 30 mW of local oscillator power[14] with limited CO_2 laser pump power.

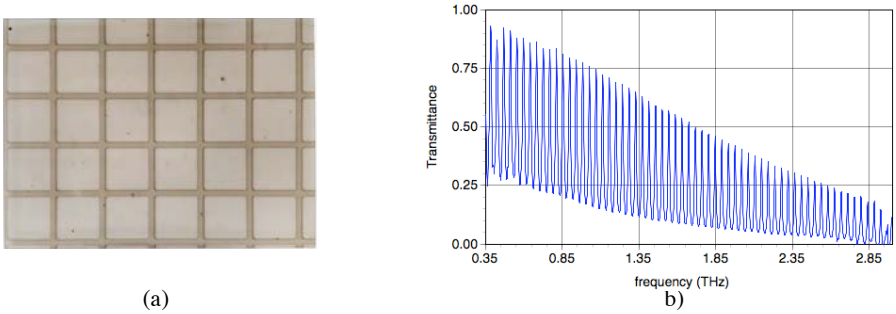

(a) b)

Figure 6. Mesh-type uniform output coupler for the 2.5 THz laser local oscillator for the NASA AURA satellite (left) and THz transmittance spectra (right).

2.4. Terahertz Resistive Sheets

The term resistive sheet typically refers to a thin film of sufficient thinness such that its complex surface impedance $Z(\omega) = R(\omega) - i\,X(\omega)$ is predominantly resistive, i.e. $R(\omega) > X(\omega)$. For a metal, this condition occurs when the skin depth δ exceeds its physical thickness t. In this case, the sheet resistance is no longer given by its infinitely thick value of $R_s = \rho/\delta$ where ρ = the metal's DC resistivity, but must be replaced by $R_s = \rho/t$. Resistive sheets are typically fabricated from carbon-loaded plastics sheets (e.g. Dupont Kapton XC).

At terahertz frequencies, resistive sheets can be fabricated by evaporating or sputtering a thin metal film onto a low loss substrate such as Mylar. An intriguing property of resistive sheets is their frequency independent optical behavior. When the condition $t < \delta$ is met, simplified expressions[15,16] for the reflected and transmitted power can be used, namely,

$$T = \left(\frac{2r'}{(1+2r')}\right)^2, \quad R = \left(\frac{1}{(1+2r')}\right)^2 \quad \text{where } r' = R_s/377. \qquad (1)$$

The frequency independent transmittance behavior of thin metal films at THz frequencies is demonstrated in Figure 7a, which shows the transmittance of several resistive sheets fabricated by evaporating metals such as chromium, inconel, and nickel onto thin Mylar sheets. Transmittance values vary from 0.9% to 93% demonstrating that a range of sheet resistances from 20 ohms/square to over 5300 ohms/square was achieved.

The data in Figure 7a display constant transmittance down to the lowest frequency measured even though δ/t is on the order of 100 at that frequency. An interesting question to ask is how low in frequency does the frequency independent behavior persist. The behavior of one of the films (49 Å Inconel on 2 micron Mylar) was investigated further. Using a 4-point resistively probe, the film's sheet resistance was measured to be $R_s \approx 295$ ohms/square. Using Eq. (1), a transmittance of 37% was predicted and is shown in Figure 7b along with measured values of the film's transmittance extending down to 10 GHz. The optical behavior of the thin metal film remains remarkably flat over the entire measured bandwidth indicating that the frequency independent behavior is valid even for very large values of δ/t.

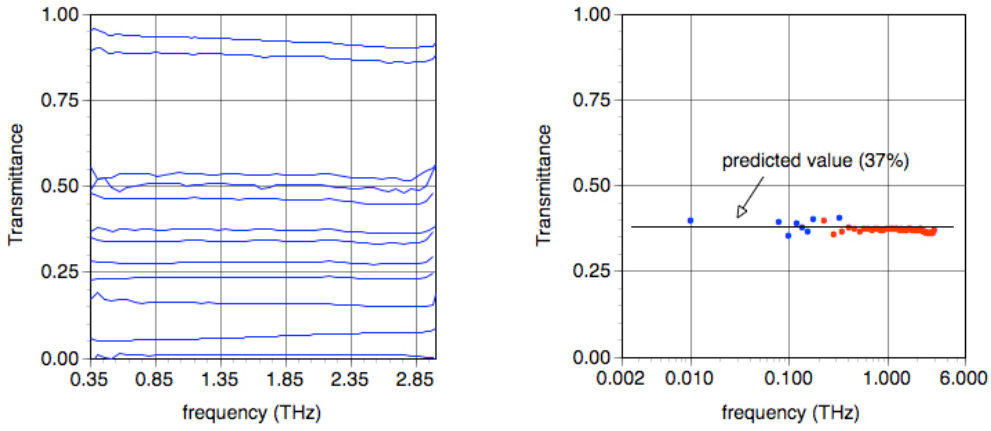

(a) (b)

Figure 7. Terahertz transmittance of several thin metallic film resistive sheets (left) and broadband frequency independence of a thin metal film's transmittance (right).

Electromagnetic absorbing materials based on resistive sheets such as Salisbury screens and Jaumann absorbers[17] are commercially available for radar frequencies. The Salisbury screen is comprised of a thin resistive layer set λ/4 apart from a thick metallic surface. For optimal performance, the sheet resistance of the thin layer is numerically equal to the impedance of free space (377 ohms). Figure 8a plots the reflectance (in dB) of a Salisbury screen operating in the terahertz region of the spectrum. The absorbing material was constructed by depositing 90 Å of Inconel ($R_s \approx 340$ ohms/square) onto a thin Mylar substrate and separating it from a thick metal surface by a 250-micron-thick polystyrene foam spacer. A null in the reflectance spectrum of less than -22 dB is observed at ≈ 0.88 THz. The null depth is directly related to the sheet resistance value of the metal film.

A variation of the Salisbury screen absorber, providing wider bandwidth capability, is known as a Jaumann absorber. These absorbers are fabricated by stacking several resistive sheets separated by λ/4-thick low-loss spacers. Figure 8b displays the reflectance spectra (in dB) of 4 and 5-layer THz Jaumann absorbers. The spacer thickness was tailored for 0.4 THz. As expected, better performance is observed for the 5-layer structure.

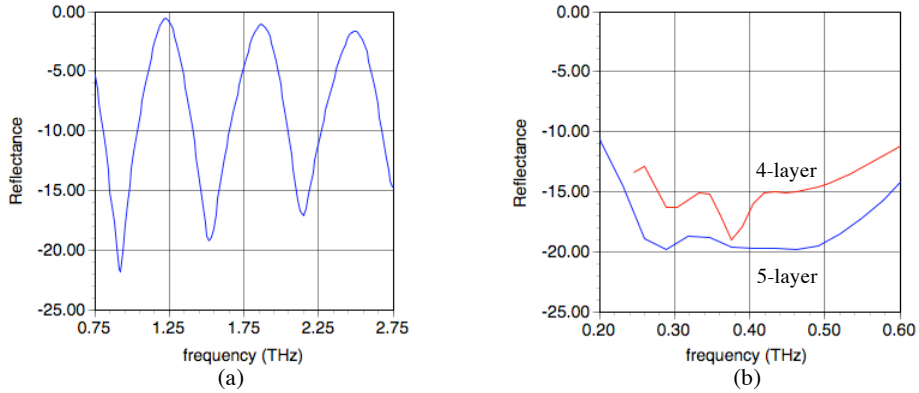

Figure 8. Reflectance of THz absorbing materials. Salisbury screen (left) and Jaumann absorbers (right).

3. TERAHERTZ PROPERTIES OF COMMON MATERIALS AND STRUCTURES

The transmittance and reflectance of a variety of building, fabric, and clothing materials at frequencies extending from millimeter waves (94 GHz) to approximately 2 THz have been measured. The work consisted of measuring the specular transmittance (T) and reflectance (R) over a continuum of frequencies from approximately 175 GHz to 2 THz using a Fourier transform spectrometer. CO_2 optically pumped THz laser lines were used to provide fixed frequency reflectance and transmittance measurements at 326 GHz, 584 GHz, and 1.04 THz and a Gunn oscillator was used for measurements at 94 GHz. All data were collected at or near normal incidence. Liquid-helium-cooled silicon bolometer detectors were used to achieve high sensitivity for both broadband and fixed frequency measurements. Fourier transform spectroscopic techniques provided approximately 20 dB of dynamic range, at 30 GHz resolution, while approximately 70 dB of dynamic range was achieved with the fixed frequency sources. The materials and structures measured are listed in Table II.

Table II. Materials and Structures Included in the Attenuation Study.

Clothing / Fabrics	Building Materials and Structures	
Cotton shirt	Concrete	Drywall
Denim	Cinderblock	Glass
Drapery	Brick	Plastic Blinds
Leather	CDX Plywood	Corrugated Cardboard
Sweater	spruce-pine-fir (SPF)	Vinyl siding on 1/2 in. CDX
Sweatshirt	oriented strand board (OBS)	Wall Section
	Maple hardwood	

In addition to individual materials, two composite structures, simulating wall construction, were built and their THz transmission was measured. The first sample is denoted as “Vinyl siding on 1/2" CDX” was approximately 1/2" thick. The second sample was built to represent a common exterior residential wall and is denoted as “Wall Section”. Figure 9 shows the cross-sectional view of the exterior wall design.

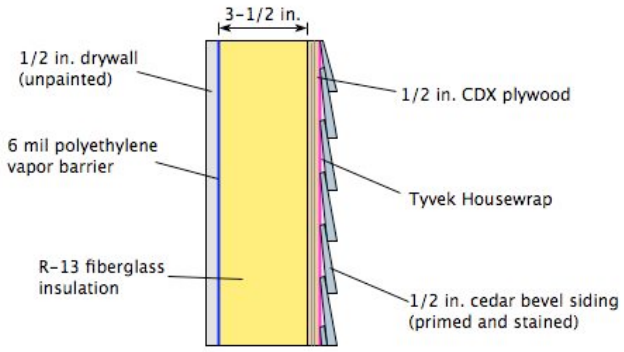

Figure 9. Cross-sectional view of the wall section constructed for the THz attenuation study.

3.1. Fixed Frequency Transmittance Data

Recognizing the inhomogeneous nature of some of the materials, a 1 in. full-width-half-maximum (FWHM) beam was chosen to illuminate the samples to provide some degree of spatial averaging. Additional averaging was obtained by measuring T at three distinct locations on the sample. Figure 10 is a schematic of the transmittance setup at 584 GHz and, with minor changes, is representative of all the fixed frequency set-ups. The 0.3 inch FWHM output beam expanded to approximately 1 inch FWHM where it was collimated by a 24-inch focal length lens. The sample was located in the center of the waist region of the collimated beam and was therefore illuminated by a planar phase front. A 3-inch diameter, 6-inch focal length lens was positioned 14 in. from the illuminated sample and focused the transmitted radiation into the bolometer. The laser beam was chopped at 100 Hz and the bolometer output, along with a chopper reference signal, was input to a lock-in amplifier.

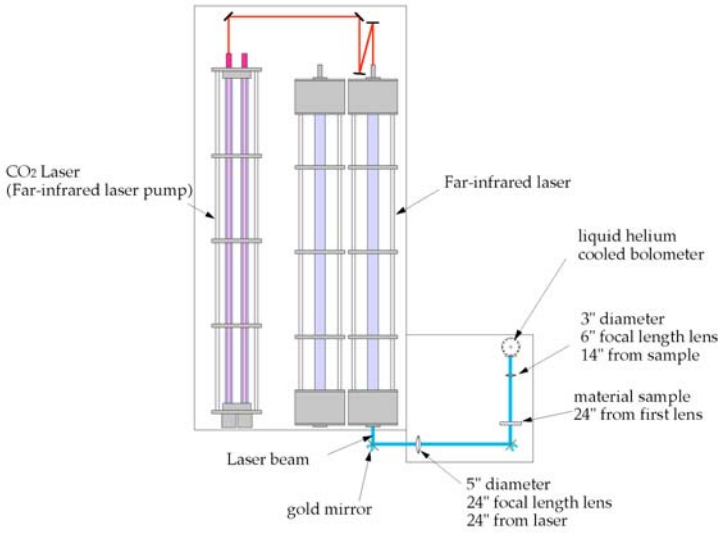

Figure 10. Schematic of the fixed-frequency transmittance measurement set-up.

The sample transmittance was defined as the lock-in amplifier output when the sample was inserted (I) to the lock-in amplifier output when the sample was removed (I_0). For convenience, we tabulated the logarithm of 1/T:

$$A_{dB} = 10 \log_{10} (I_0/I), \qquad (2)$$

and called this the attenuation. It was anticipated that certain materials, such as wood, would be anisotropic as well as inhomogeneous. To obtain a more complete characterization of the materials, measurements were made of the attenuation for the E-field both parallel and perpendicular to a (approximate) symmetry direction in the sample. For example, the symmetry direction was chosen to be parallel to the grain lines in the wood samples. The radiation output was linearly polarized in the vertical direction, so the measurements were made with the symmetry direction in the vertical direction (parallel attenuation) and with the sample rotated 90 degrees (perpendicular attenuation). A summary of material attenuation values found using fixed frequency techniques is given in Table III.

Table III. Attenuation Values for Clothing, Fabric, and Building Materials.

Values are expressed in dB.

		94 GHz		326 GHz		584 GHz		1042 GHz	
material	thick. (inches)	parallel	perp.	parallel	perp.	parallel	perp.	parallel	perp.
COTTON SHIRT	0.012	0.2	0.1	0.3	0.5	1.0	1.1	3.1	3.2
DENIM	0.025	0.7	0.7	1.3	1.4	3.4	2.9	10.0	7.9
DRAPERY	0.035	0.3	0.5	3.0	1.7	7.5	7.6	12.3	11.4
LEATHER	0.051	0.7	0.6	2.3	2.1	6.0	5.2	17.9	15.3
SWEATER	0.084	0.4	0.4	3.8	4.0	14.5	13.7	19.1	21.4
SWEATSHIRT	0.082	0.3	0.2	0.8	1.1	4.3	3.8	14.3	13.9
CARDBOARD	0.155	1.2	1.3	2.8	3.2	4.4	5.0	9.0	9.4
MAPLE 1	0.125	2.6	1.8	8.4	5.3	16.2	11.0	n/m	n/m
MAPLE 2	0.25	5.9	4.0	20.1	16.0	31.4	22.7	65.7	52.4
MAPLE 3	0.5	10.8	7.1	32.4	22.5	62.6	45.9	n/t	n/t
MAPLE 4	0.762	16.9	10.4	48.0	33.1	n/t	68.4	n/t	n/t
MAPLE 5	0.762	16.6	9.5	46.5	31.0	n/t	62.7	n/t	n/t
OSB 1	0.25	6.4	7.1	33.2	33.4	47.8	48.2	n/t	n/t
OSB 2	0.5	20.6	18.9	59.4	55.8	n/t	n/t	n/t	n/t
PLYWOOD 1	0.25	5.3	4.5	18.2	16.7	31.3	30.2	n/t	61.9
PLYWOOD 2	0.5	8.7	10.8	30.3	30.4	31.3	30.2	n/t	n/t
SPF1	0.125	3.0	1.7	7.2	4.9	14.3	9.3	29.2	20.7
SPF2	0.25	4.8	2.8	14.0	8.5	24.5	15.9	56.5	38.4
SPF3	0.5	10.8	5.8	28.8	19.2	55.9	38.4	n/t	n/t
SPF4	0.74	15.8	9.6	42.6	27.3	53.3	72.0	n/t	n/t
SPF5	0.985	21.0	12.3	55.3	35.8	n/t	74.0	n/t	n/t
SPF6	1.43	30.2	18.7	70.4	54.4	n/t	n/t	n/t	n/t
CONCRETE	0.438	9.8	10.5	47.7	49.2	n/t	n/t	n/t	n/t
DRYWALL	0.375	1.6	1.7	10.7	10.5	35.2	35.0	n/t	n/t
DRYWALL	0.5	2.2	2.8	12.8	13.1	49.1	50.4	n/t	n/t
GLASS	0.087	4.5	4.3	10.8	11.0	25.3	25.4	n/t	n/t
PLASTIC BLIND	0.033	0.5	0.5	1.3	1.4	3.6	3.4	8.2	8.1
VINYL SIDING	0.042	0.7	0.8	2.5	2.3	5.4	5.4	12.6	11.4
VIN. SID. & 1/2" CDX	0.512	10.8	12.6	32.5	32.5	68.1	68.2	n/t	n/t
WALL SECTION	4.768	17.9	22.1	69.0	70.6	n/t	n/t	n/t	n/t
BRICK1	0.452	8.7	8.9	62.7	64.3	n/t	n/t	n/t	n/t
BRICK2	0.595	15.1	16.3	n/t	n/t	n/t	n/t	n/t	n/t
BRICK3	0.252	5.4	6.1	39.9	40.3	n/t	n/t	n/t	n/t
BRICK4	0.206	5.9	5.7	n/m	n/m	n/t	n/t	n/t	n/t
BRICK9	0.338	7.1	6.7	46.9	50.0	n/t	n/t	n/t	n/t
CINDER BLOCK 1	1.091	45.9	48.3	n/m	n/m	n/t	n/t	n/t	n/t
CINDER BLOCK 5	0.331	16.5	16.5	53.1	53.1	52.8	56.8	n/t	n/t
CINDER BLOCK 7	0.385	17.7	17.4	54.1	52.7	62.3	60.6	n/t	n/t
CINDER BLOCK 9	0.67	26.6	26.9	74.7	75.6	n/t	n/t	n/t	n/t

n/t-no transmission
n/m- no measurement

Certain clothing, fabric, and building materials studied are probably inhomogeneous on the terahertz wavelength scale. Therefore, it was suspected that some portion of the measured attenuation in building materials was due to scattering and therefore an additional measurement at 584 GHz was conducted to demonstrate this. If the transmission loss were entirely due to electromagnetic absorption, then the measured value of A_{dB} would be independent of the sample position along the beam path; but if any scattering effects were present, the transmittance would increase when the receiver collection angle, subtended by the sample, was made larger. A cinderblock and the plastic blind (the latter presumed to be a homogeneous material) were measured in the standard position as well as directly in front of the bolometer input window, to maximize the receiver collection angle. The results, shown in Table IV, are consistent with the notion that radiation scattering contributed to the measured values of A_{dB} in certain materials.

Table IV. Comparison of Attenuation Values for Homogenous and Inhomogeneous Materials.

material	thickness (inches)	Sample placed in normal sample position	Sample placed at bolometer
cinderblock (parallel atten.)	0.385	63.1 dB	53.8 dB
plastic blinds (parallel atten.)	0.033	3.6 dB	3.6 dB

3.2. Broadband Reflection and Transmission Data

In addition to measurement of material attenuation data at several fixed frequencies, the specular transmittance and reflectance of the materials were measured using a Fourier transform spectrometer. Transmission measurements were performed at normal incidence and reflectance measurements were performed at an angle of incidence of ≈ 15°. Just as for the fixed frequency measurements, R and T were measured for the electric field of the polarized beam both parallel and perpendicular to a chosen symmetry direction in the material. Data were generally in very good agreement with the fixed-frequency results. Transmittance data for several of the clothing and building materials are shown in Figure 11. It is interesting to note that the terahertz region of the spectrum appears to be a region where several common materials transition from generally transparent to opaque behavior.

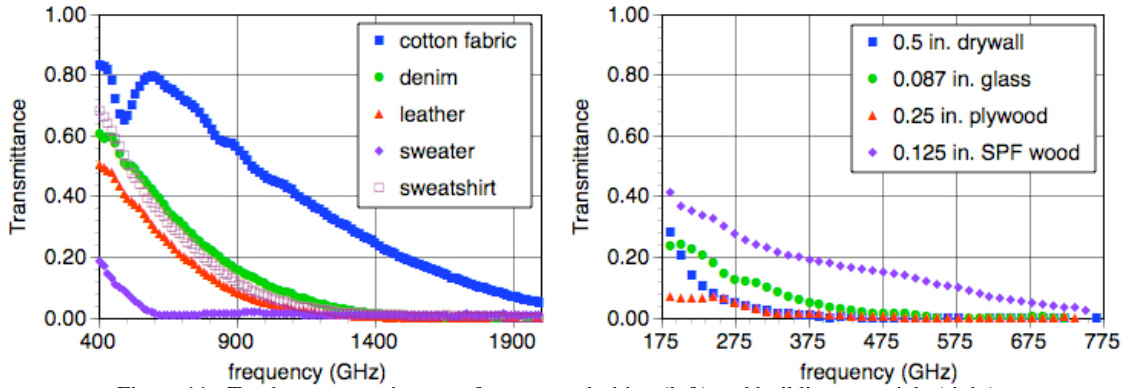

Figure 11. Terahertz transmittance of common clothing (left) and building materials (right).

Clothing and fabrics should diffract terahertz radiation, since the periodicity, d, of the weave pattern is typically in the hundreds-of-microns range. The transition from non-diffractive to diffractive behavior occurs when the wavelength becomes smaller than the periodicity. In the transition region, abrupt changes in the material's transmittance may occur and R should decrease as λ transitions from the long to short wavelength side of d. Qualitatively, this behavior is observed in the measurements. The cotton fabric sample, which had the cleanest weave pattern (d ≈ 560 micron) of any of the materials studied, exhibited an abrupt change in transmittance and decrease in reflectivity near λ = 560 micron (535 GHz). The phenomenon is shown in Figure 12a below.

The anisotropy of several of the materials had a noticeable effect on their THz behavior. This effect is observable in many of the data in Table III. Figure 12b shows the transmittance of leather (assumed isotropic) and SPF wood (assumed anisotropic). Leather's parallel and perpendicular transmittance data shows no appreciable polarization dependence, however, the data for SPF wood shows substantial polarization dependence.

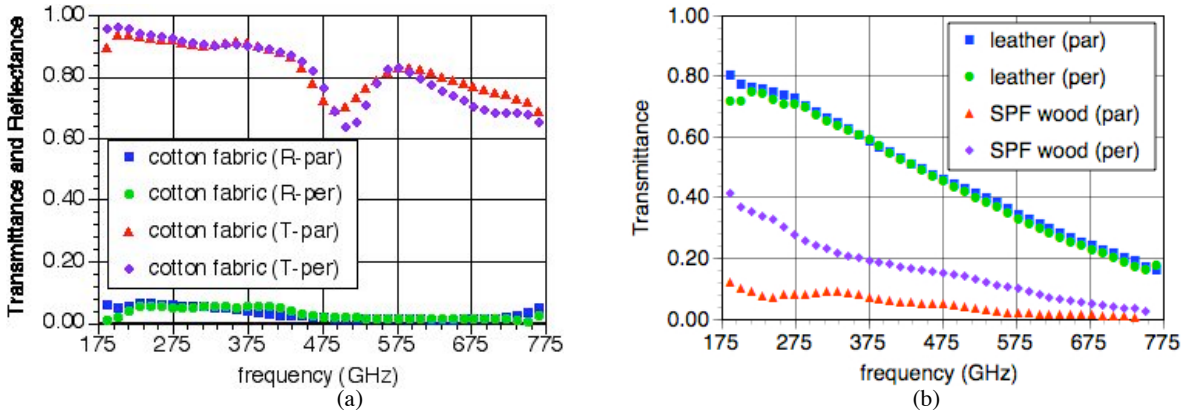

Figure 12. Terahertz transmittance and reflectance of cotton fabric displaying evidence of diffraction (left) and the behavior of isotropic and anisotropic materials (right).

4. CONCLUSION

The behavior of several components such as bandpass filters, output couplers, artificial dielectrics, and resistive sheet absorbers and their application in the terahertz region of the spectrum were discussed. Transmission and reflection measurements in the spectral range from 94 GHz to 2 THz were also presented on clothing, fabric, and building materials. A variety of terahertz materials characterization systems were utilized to collect the data including a broadband Fourier transform spectrometer as well as fixed-frequency sources. The data presented here are being compiled into a more extensive THz optical properties database available to government agencies and their contractors upon request.

ACKNOWLEDGEMENTS

This work was supported by the National Ground Intelligence Center under Army contract DASC-01-01-C-0011 and by MIT Lincoln Laboratory under Air Force Contract F19628-00-C-0002. Opinions, interpretations, conclusions, and recommendations are those of the authors and are not necessarily endorsed by the United States Government.

REFERENCES

1. C. Beaudoin, A. Gatesman, R. H. Giles, J. Waldman, and W. E. Nixon, "Generation of High-Resolution 3D UHF SAR Imagery Using a Physical Scale Modeling Approach," Proceedings of SPIE Vol. 6237 *Algorithms for Synthetic Aperture Radar Imagery XIII*, edited by E. G. Zelnio and F. G. Garber, (SPIE, Bellingham WA, 2006).

2. M. J. Coulombe, T. Horgan, J. Waldman, J. Neilson, S. Carter, and W. Nixon, "A 160 GHz Polarimetric Compact Range for Scale Model RCS Measurements," Antenna Measurements and Techniques Association (AMTA) Proceedings, Seattle, WA, October 1996.

3. T. M. Goyette, J. C. Dickinson, C. Beaudoin, A. J. Gatesman, R. H. Giles, J. Waldman, and W. E. Nixon, "Acquisition of UHF and X-Band ISAR Imagery Using 1/35th Scale Models," Proceeding of SPIE Defense and Security Symposium, Vol. 5808, Orlando, FL, March 2005.

4. M. J. Coulombe, T. Horgan, J. Waldman, G. Statkowski, and W. Nixon, "A 520 GHz Polarimetric Compact Range for Scale Model RCS Measurements," Antenna Measurements and Techniques Association (AMTA) Proceedings, Monterey, October 1999.

5. T. M. Goyette, J. C. Dickinson, J. Waldman, W. E. Nixon, and S. Carter, "Fully Polarimetric W-band ISAR Imagery of Scale-Model Tactical Targets Using a 1.56 THz Compact Range," Proceeding of SPIE 15th Annual Inter. Symp. on Aerospace/Defense, Simulation, and Controls, Vol. 4382, Orlando, FL, April 2001.

6. A. J. Gatesman, T. M. Goyette, J. C. Dickinson, J. Waldman, J. Neilson, and W. E. Nixon, "Physical Scale Modeling the Millimeter-Wave Backscattering Behavior of Ground Clutter," Proceeding of SPIE 15th Annual Inter. Symp. on Aerospace/Defense, Simulation, and Controls, Vol. 4370, Orlando, FL, April 2001.

7. C. Winnewisser, F. Lewen, and H. Helm, "Transmission Characteristics of Dichroic Filters Measured by THz Time-Domain Spectroscopy," Appl. Phys. A 66, pp. 593-598 (1998).

8. M. MacDonald, A. Alexnian, R. A. York, Z. Popovic, and E. N. Grossman, "Spectral Transmittance of Lossy Printed Resonant-Grid Terahertz Bandpass Filters," IEEE Trans. Microwave Theory Tech. vol. 48, no. 4, pp. 712-718, April 2000.

9. D. W. Porterfield, J. L. Hesler, R. Densing, E. R. Mueller, T. W. Crowe, and R. M. Weikle, "Resonant Metal-Mesh Bandpass Filter for the Far-Infrared," Appl. Opt. vol. 33, no. 25, pp. 6046-6052, Sept. 1994.

10. A. J. Gatesman, R. H. Giles, and J. Waldman, "A High-Precision Reflectometer for Submillimeter Wavelengths," J. Opt. Soc. Am. B/Vol. 12, No. 2, Feb. 1995.

11. R. Densing, A. Erstling, M. Gogolewski, H Gemund, G. Lundershausen, and A. Gatesman, "Effective Far Infrared Laser Operation with Mesh Couplers," Infrared Physics, Vol. 33, No. 3, pp. 219-226, 1992.

12. L.W. Henderson, *Introduction to PMM, Version 4.0*, Technical Report 725347-1, Contract No. SC-SP18-91-0001, The Ohio State University ElectroScience Laboratory, Columbus, OH, July 1993.

13. W. A. Bailey, A. J. Gatesman, K. R. Gingras, and W. D. Goodhue, "Fabrication and Optimization of Uniform Output Couplers for Far-infrared Lasers," Optics Letters, Vol. 25, No. 18, pp. 1349-1351, Sept. 2000.

14. B. D. Johnson, "Laser System to Map Ozone Depletion," Photonics Spectra, April, 2003.

15. J. Stratton, *Electromagnetic Theory*, McGraw-Hill, (1941).

16. C. A. Klein, "Microwave Shielding Effectiveness of EC-Coated Dielectric Slabs," IEEE Trans. Microwave Theory and Tech, Vol. 38, No. 3, pp. 321-324, March 1990.

17. E. Knott, *Radar Cross Section*, 2nd Edition, Artech House, (1993).